Hindawi
Complexity
Volume 2020, Article ID 8873876, 13 pages
https://doi.org/10.1155/2020/8873876

Research Article

Optimization of Wheel Reprofiling Based on the Improved NSGA-II

Xinghu Wang, Jiabin Yuan, Sha Hua, and Bojia Duan

College of Computer Science and Technology, Nanjing University of Aeronautics and Astronautics, Nanjing 210016, China

Correspondence should be addressed to Xinghu Wang; tiger@nuaa.edu.cn

Received 10 August 2020; Revised 9 November 2020; Accepted 4 December 2020; Published 23 December 2020

Academic Editor: Zhile Yang

Wheels are the key components of a train, and the shape of the wheel flange should be maintained to ensure the security of train operations. As a method to maintain the shape at the cost of the diameter size, reprofiling has significant impacts on the lifecycle of a train. A wheel model is built in this paper based on the analysis of the wheel wear features and datasets from Taiyuan locomotives. With the decision variables (T_i, T_i'), which describe the reprofiling strategy, we formulate a multiobjective optimization problem simultaneously minimizing the reprofiling numbers and maximizing the serving years. To find the solutions of the multiobjective model, the NSGA-II (nondominated sorting genetic algorithm II) is extended with an alteration of the crowding distance calculation and genetic operators. The improved NSGA-II performs better than other approaches (e.g., fixed reprofiling strategy, changeable reprofiling strategy, and NSGA-II). Meanwhile, outstanding solutions with longer servicing years and less reprofiling are listed in this paper. Our study reveals the relationship between the diameter, flange thickness, and their individual attrition rates and proposes a wear model, multiobjective model, and improved NSGA-II. Compared with existing reprofiling strategies, the strategy recommended in our work can significantly increase the lifecycle of the wheel coupled with a low repair frequency.

1. Introduction

In recent years, Chinese railway construction has entered a new stage of rapid development. According to the ministry's annual statistical bulletin, the running mileage of railways reached 127,000 kilometers in 2017. More than 23,000 kilometers of new railway lines will be constructed during the thirteenth Five-Year Plan, and the total investment will be beyond 2.8 trillion CNY. However, with the continuous operation of the train, the cost of reprofiling takes up a large proportion of the maintenance cost, e.g., approximately 8 billion CNY per year. Thus, maintenance optimization techniques for the railway system are required under the rapid growth of rail transportation.

Wheels are the key components of a train, and their health status is closely related to the safety, comfort, and smoothness of train operations. Minor changes in the wheels may cause train accidents. The aim of wheel reprofiling is to process the worn wheels to the geometric size of the standard contour. If such worn wheels continue to be used, there will be an increased danger of derailment.

Engineers develop most of the wheel maintenance strategies through experience. To improve the flexibility, there has been increasing interest in the area of optimizing maintenance strategies over recent decades. Fires R H and Dfivial C G built a prediction model based on the multibody dynamics and concluded that the wheel wear model in direct proportion to the law force is the best [1]. Roger Enblom and Mats Berg investigated the wear distributions over nonelliptic patches under different operating conditions and simulated on the theory of vehicle track coupling dynamics [2]. Xu built a wheel wear model for the metro train based on the Gauss method and provided an optimizing policy for wheel repair [3]. Dirks and Enblom described the differences between the wear and RCF prediction models and showed that adjustments of the models have a significant influence on the RCF prediction [4]. Ding et al. simulated the wheel wear of a heavy haul freight car based on the FASTSIM algorithm and Zobory

tread wear model [5]. With the combination of the vehicle dynamics and the wheel profile parameters, Zhang et al. presented a new approach to optimize reprofiling decisions [6]. According to the wheelset maintenance data of a certain type of urban rail train, Liao acquired the optimal recovery threshold of the flange thickness through a linear regression analysis of the flange wear and flange thickness [7]. Wang et al. developed a data-driven model and listed the preferred reprofiling strategies for the Guangzhou Metro Line One [8].

These papers indeed discussed the optimization problem of wheel maintenance strategies, but there are two main shortcomings. On the one hand, most existing strategies rely on vehicle dynamics, and various modern algorithms have not been applied to this field. On the other hand, plenty of data that contain rich information have not been fully exploited. Few studies have taken serving years and the repair frequency of a wheel into consideration together.

Multiobjective evolutionary algorithms (MOEAs) are widely used in multiobjective optimization problems. The current mainstream multiobjective evolutionary algorithm mainly includes NSGA-II (nondominated sorting genetic algorithm II) [9], SPEA (strength Pareto evolutionary algorithm) [10], SPEA2 (strength Pareto evolutionary algorithm 2) [11], etc. These algorithms simulate genetic methods in nature, through iteration from parent to children in the direction of optimal solution, to give a final solution of the problem.

Although many MOEAs have been proposed, most researchers agree that few of these approaches have been adopted as a reference. Meanwhile, the NSGA-II is a paradigm within the MOEA research community for the powerful crowding operator. The NSGA-II [12] is based on the GA to solve multiobjective optimization problems. It will first generate a random parent population of size nPop. Then, a new population with genetic operators is created, and the generated offspring is ranked together with the parents with the nondominated sorting procedure. Each solution is assigned a fitness value (or rank value) equal to its nondominated level. The crowding distances between members on each front are calculated. Finally, the next-generation individuals of the population size and the procedure will be continued until the maximum number of cycles is reached.

To overcome the above limitations about the wheel maintenance strategies, this paper makes the following contributions:

(1) Definition and models: the actual wheel reprofiling problem is formulated as a mathematical problem, and the wear model and multiobjective optimization model are established.

(2) Improved NSGA-II: the NSGA-II is extended in the elite individual selection strategy and the genetic operators to better fit the proposed multiobjective model.

The reminder of this paper is organized as follows. In Section 2, the definition of the problem is given. Then, the mathematical wear model is stated, and the multiobjective model is proposed. Section 3 presents the improved NSGA-II algorithm. Numerical experiments and results are shown and compared in Section 4, while the conclusions and future studies are given in Section 5.

2. Definitions and Models

The flange height, flange thickness, flange gradient, wheel diameter, and QR value are all parameters that describe a wheel. The flange thickness and the wheel diameter are the two most significant measurements for wheels. Therefore, this work considers these two variables as the key components.

2.1. Problem Definition. Reprofiling is the main method of maintenance during the lifecycle of a wheel. As shown in Figure 1, the wheel diameter will be reduced during the reprofiling process to recover the original shape of the wheel, and the flange thickness will increase. The reprofiling gain k, also called the turning gain [13], is defined as follows:

$$k = \frac{\Delta D}{\Delta T}, \tag{1}$$

where ΔD is the wheel diameter loss in the reprofiling process and ΔT is the gained flange thickness. A value of 4.2 is utilized as the turning gain in this paper [14].

As mentioned above, a wheel should be reprofiled as soon as possible when the flange thickness is less than the minimum allowable value. Thus, in the daily operations of a train, the reprofiling problem is related to a decrease in the wheel diameter and an increase in the flange thickness. Additionally, the wheel must be replaced once the diameter is less than the threshold of 1150 mm.

To better delimit the problem, the flange thickness T is considered the process variable, which is used to control the reprofiling process. The wheel diameter D is used as the terminate variable, which represents the end of the wheel lifecycle.

It is assumed that the i-th reprofiling strategy is (T_i, T_i'), where T_i is the flange thickness before reprofiling and T_i' is the flange thickness value after reprofiling. If the entire lifecycle of a wheel contains N reprofilings, then all the reprofiling strategies of a wheel can be expressed as (T_1, T_1'), (T_2, T_2'), ..., (T_i, T_i'), ..., (T_N, T_N').

Since the object of this work is a locomotive of type SS4-0997, the flange thickness begins at 34 mm, and the minimum threshold is 28 mm. Meanwhile, D begins at 1250 mm and ends at 1150 mm. When considering the entire life of the wheel, the flange thickness begins from 34 mm and will undergo repeated (T_i, T_i') processes until the diameter is less than 1150 mm. Assuming that the flange thickness before the wheel scrapped is T_{end}, the entire lifecycle of a wheel is given as $(34, T_1)$, (T_1', T_2), ..., (T_{i-1}', T_i), ..., (T_N', T_{end}).

Therefore, the reprofiling problem is abstracted into finding (T_i, T_i'), where N is the minimum and the serving years are the maximum.

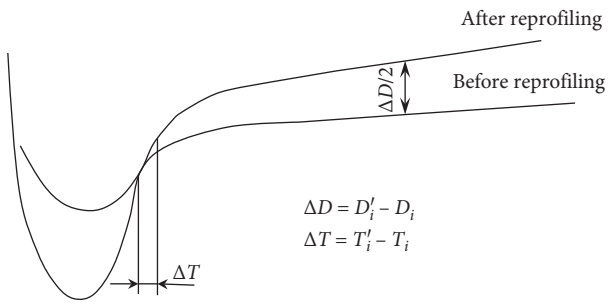

Figure 1: Reprofiling procedure.

2.2. Models. With the definition of the wheel reprofiling problem, the wear model and multiobjective model are built.

2.2.1. Wear Model. Datasets from the SS4-0997 train from the Taiyuan North Locomotive Depot are used to study the wear regularity. We eliminate the dirty data according to the FSFDP proposed by Alex in 2014 [15]. Considering the preprocessing data, the variations in the wheel diameter and flange thickness are defined as follows:

$$v_d = \frac{D_{t_{i+1}} - D_{t_i}}{t_{i+1} - t_i} * 5, \tag{2}$$

$$v_t = \frac{T_{t_{i+1}} - T_{t_i}}{t_{i+1} - t_i} * 5, \tag{3}$$

where 5 is taken as a test unit for the interval of the Tycho examination machine, which is relatively short. The value of the diameter tested on day t_i is symbolized as D_{t_i}, and v_d is the abrasion rate of the wheel diameter. The T_{t_i} in equation (3) represents the value of the flange thickness tested on day t_i, while v_t is the wear rate of the thickness between t_i and t_{i+1}. The correlative coefficients are calculated to reveal the relationships between D, T, v_d, and v_t. The computational results in Table 1 show that v_d is closely related to D (resp. −0.1225), and v_t is correlated with T (resp., −0.2041). With the correlation coefficient of −0.0422 and a significance level of 0.05, v_d is independent from T, which is the same for v_t and D (resp., 0.0504).

The wheel diameter and the flange thickness are both divided into segments of 0.1 millimeters in which the averages of v_d and v_t are calculated. The quadratic curve fitting method based on a weighted least squares is applied to determine the relationships between D and v_d and between T and v_t. The fitting curves are plotted in Figure 2, and the expressions are given as follows:

$$\begin{aligned} v_d &= -0.00621 * D^2 + 15.4 * D - 9544.0, \\ v_t &= -0.0262 * T^2 + 1.64 * T - 25.7. \end{aligned} \tag{4}$$

Figure 2(a) is the fitted curves of the wear rate of the wheel diameter. The abscissa is the wheel diameter value, the ordinate is the wear rate, the blue asterisk is the calculated discrete value of the wear rate, and the red curve is the fitted curve. It can be seen from Figure 2(a) that when the wheel diameter is 1239.94 mm, the wear rate is the smallest, which is close to zero. Correspondingly, Figure 2(b) is the fitting curve of the wear rate of flange thickness. When the flange thickness is 31.2 mm, the wear rate is the slowest. Comparing the fitting effects of the two figures, it can be clearly seen that Figure 2(a) is better. The following error analysis is based on the above fitting results.

The errors between the real data and fit data are calculated to increase the accuracy of this work. As shown in Figure 3(a), the error in the wheel diameter follows a normal distribution with mean 0 and standard deviation 1.28, as in equation (5). In Figure 3(b), the flange thickness is divided into three segments: [28, 29.5], [29.5, 33], and [33, 34], as in equation (6):

$$\text{Error1} \sim N(0, 1.28), \tag{5}$$

$$\text{Error2}(T) = \begin{cases} 0.8981 * T^2 - 53.5456 * T - 797.6447, & T \in [28.0, 29.5], \\ -0.0347 * T^2 + 2.1169 * T - 32.3036, & T \in [29.5, 33.0], \\ -2.4 * T^2 + 162.8 * T - 2709.4, & T \in [33.0, 34.0]. \end{cases} \tag{6}$$

The wear functions of the wheel diameter and flange thickness become

$$\begin{aligned} v_d &= -0.00621 * D^2 + 15.4 * D - 9544.0 + \text{Error1}, \\ v_t &= -0.0262 * T^2 + 1.64 * T - 25.7 + \text{Error2}. \end{aligned} \tag{7}$$

Coupled with these functions, we can assume that the wheel wear process starts from the original flange thickness of 34 millimeters and ends at 28 millimeters based on the wear rate of function v_t. The wheel diameter abrades from 1250 millimeters with the rate of v_d until 1150 millimeters.

2.2.2. Multiobjective Model of the Wheel. With the definition of the reprofiling problem, the serving years of each unit (T_i, T_i') can be obtained from the wear functions above, which is expressed as $f(T_{i-1}', T_i)$. The total serving years of a wheel can be expressed as the summation of each reprofiling unit. Thus, the first objective function is expected to be the maximum and is stated as

$$\max Y = f(34, T_1) + \sum_{i=1}^{N-1} f(T_{i-1}' - T_i) + f(T_N', 28). \tag{8}$$

Table 1: Correlative coefficient.

-	Wheel diameter (D)	Flange thickness (T)
v_d	−0.1225	−0.0422
v_t	0.0504	−0.2041

In addition, the reprofiling numbers are considered to be small enough to minimize the losses of the wheel diameter. The entire lifecycle of a wheel contains $N + 1$ units, so the second objective function is expressed as follows:

$$\min F = N + 1. \tag{9}$$

There are several restrictive conditions in the model. First, the wheel diameter should be in the range of [1150 and 1250], while the flange thickness should fall in [28, 34]. Second, the reprofiling strategy (T_i, T_i') must follow the rule $T_i < T_i'$. Finally, the adjacent repair strategies should follow $T_{i-1}{}' < T_i$. Coupled with the objective functions and restrictions, the multiobjective reprofiling model of a wheel is presented in equation (10) and is transformed into equation (11) to make the objective functions uniform:

$$\begin{aligned} &\max, Y, \\ &\min, F, \\ &\qquad 1150 \le D_i \le 1250, \\ &\text{subject to} \quad 28 \le T_i \le 34, \\ &\qquad T_i < T_i', \end{aligned} \tag{10}$$

$$\begin{aligned} &\min, (-Y, F), \\ &\qquad 1150 \le D_i \le 1250, \\ &\text{subject to,} \quad 28 \le T_i \le 34, \\ &\qquad T_i < T_i'. \end{aligned} \tag{11}$$

3. The Improved NSGA-II Approach

Based on the NSGA-II, a new approach to solve the multiobjective problem is proposed. The global density is first introduced to overcome the limitation of the crowding distance in the classical NSGA-II. Additionally, new genetic operators are proposed to better apply the multiobjective presented in Section 2.2.2.

3.1. Crowding Distance Calculation. In the traditional NSGA-II, the crowing distance is the average of two points on either side of this point along each of the objectives. As shown in Figure 4(a), the crowding distance of i in its front is the average side length of the cuboid (shown with a dashed box).

Since the density calculation of the classical NSGA-II is limited to a single layer, the distance calculation cannot precisely measure the density of point i. Taking Figure 4(b) as an example, the classical calculation shows that the crowding distance of points c and d is the same. However, the density of point c (including points 3, 4, a, b, and d) is larger than that of d (points 5, 6, and e). Therefore, in terms of the global density, point c will be better than point d, and the global density is introduced here to overcome the drawbacks above.

With a large population size, the discrete distances are prone to conflict with each other. To obtain continuous values, the Gaussian kernel equation (12) is chosen to find the density in this paper, where $\|x - xc\|$ is the distance from point x to the target point x_c, and dealt is the kernel width:

$$f(x) = e^{-\left((x - x_c^2)/(2\delta)^2\right)}. \tag{12}$$

Equation (11) is transformed into equation (13) to better fit the calculation of the global crowding distance:

$$d_i = \sum_{j \in I_S/\{i\}} e^{-\left(d_{ij}/d_c\right)^2}, \tag{13}$$

where d_c is the cutoff distance, which is defined by the users, and d_{ij} is the distances of all points i to the target point i. Therefore, the crowding distance is the sum of the Gaussian distances of all the points to the target point.

For the cutoff distance d_c, we may choose the distance that causes the average number of each targets' adjacent points less than the cutoff distance to account for 1% of all the data points.

With the calculation of the global crowding distance and the fast nondominated sorting approach of the NSGA-II, each individual will have two attributes as follows:

(1) Nondominated rank of the NSGA-II: i_{rank}

(2) Density value: $i_{\text{density}} = \rho_i$

The population is ranked based on the nondomination sorting procedure of the NSGA-II, which is marked as attribute 1 (individuals in the first front achieve the smallest rank). The density value (attribute 2) between members in the entire population is then calculated using the Gaussian kernel. Solutions with lower ranks will be chosen first, and individuals with a smaller ρ_i will be selected in advance when solutions belong to the same front.

3.2. Genetic Operators. This section discusses improvements to the corresponding genetic operators of the classic NSGA-II to solve the problem mentioned in Section 2.

3.2.1. Selection Operator. Binary tournament selection, which is a random method to select individuals in parents, is used in the NSGA-II. However, in our work, the second fitness value is expected to be small enough to reduce the reprofiling costs, while the using years are expected to be larger. Therefore, the individuals we choose are mainly concentrated at the bottom. To accurately distinguish the individuals, the k-means classification algorithm is used first in the choice operation.

Figure 5 shows the result of using the k-means algorithm. The green points are those we prefer to choose (Part A), and then, the red and blue ones are Part B and Part C, respectively. The three parts are all chosen to guarantee diversity in the population.

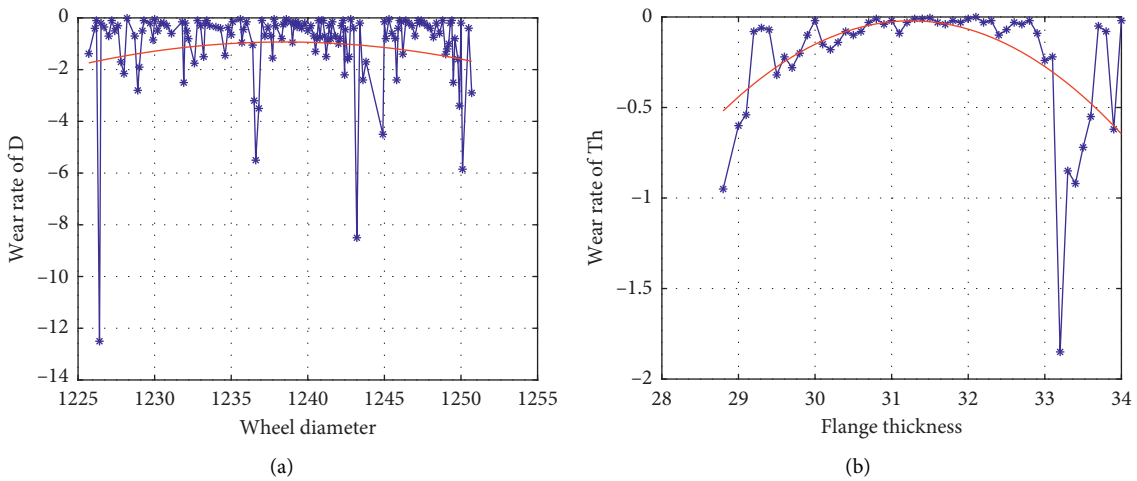

Figure 2: Fitted curves: (a) the wear rate of wheel diameter; (b) the wear rate of flange thickness.

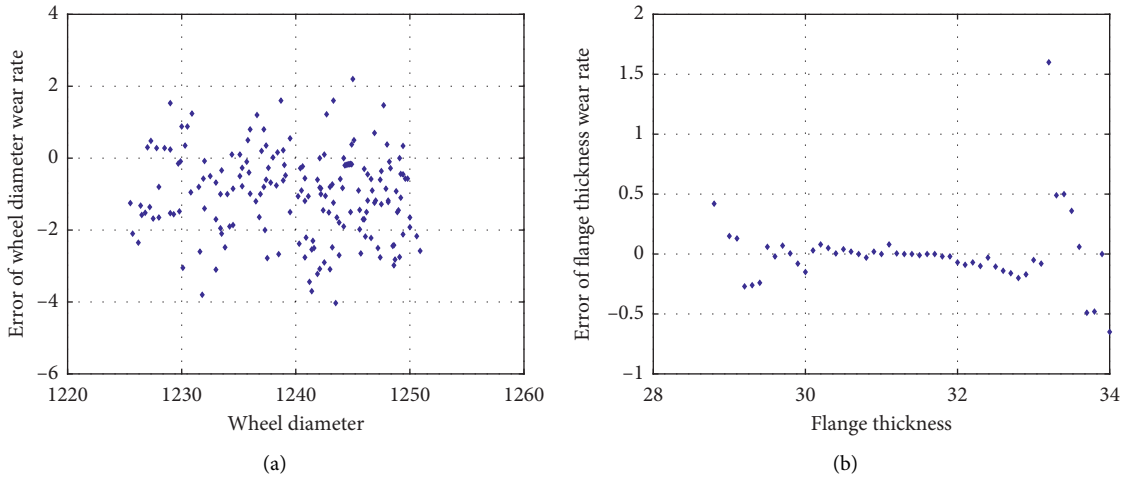

Figure 3: Error points chart of wear rate: (a) wheel diameter; (b) flange thickness.

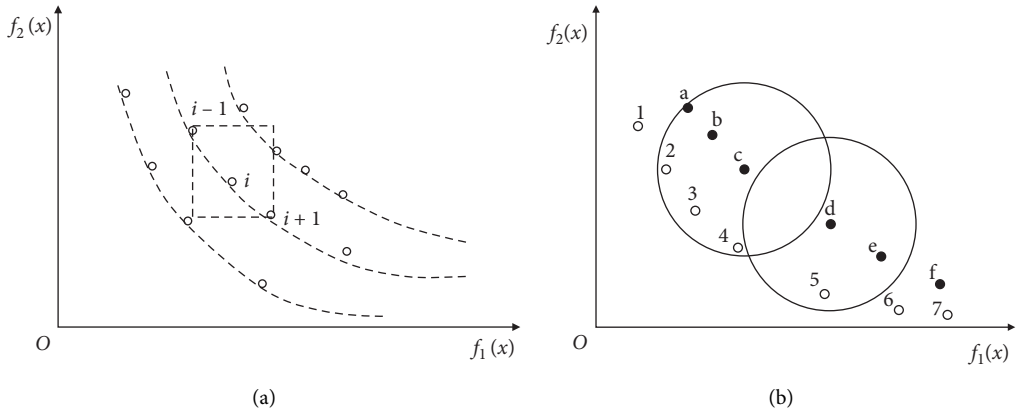

Figure 4: Density calculation diagram. (a) Crowding distance of the NSGA-II. (b) Density of points.

Figure 6 provides details of the specific selection process. The father population will be divided into A, B, and C parts, where class A is the main selection object whose size might be half of the total population *n*Pop. The remaining individuals are equally distributed in B, C, and A; B and A; and C, B, and C. The method not only retains superior parents

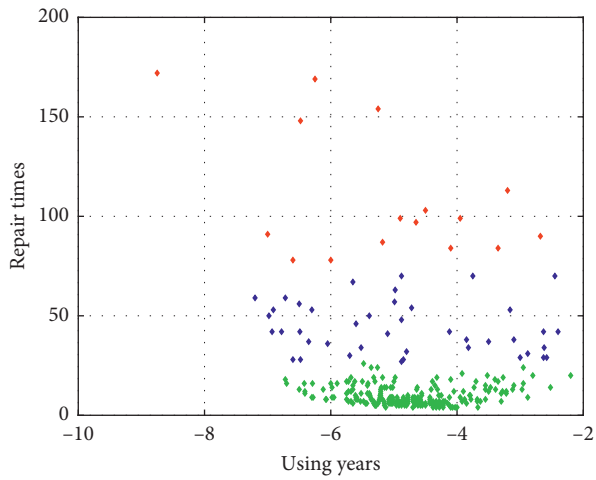

Figure 5: Classification of the datasets.

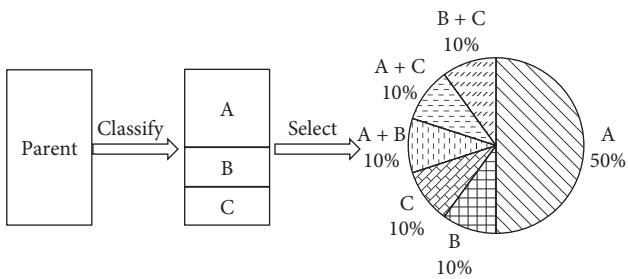

Figure 6: Population selection process.

with low reprofiling times but also ensures the diversity of the population.

3.2.2. Crossover Operator. The crossover operator is used to explore a new solution space and vary the population from one generation to the next. The SBX crossover operator in equation (14) and equation (15) in the NSGA-II will propagate the best qualities to the next generation. However, with a fixed α (the arithmetic crossover operator), the global search ability is a little weaker:

$$X_A^{t+1} = \alpha X_A^t + (1-\alpha) X_B^t, \tag{14}$$

$$X_B^{t+1} = (1-\alpha) X_A^t + \alpha X_B^t. \tag{15}$$

A new crossover operator equation (16) and equation (17) is defined in our work to take the quality of individuals into consideration. In this way, in the early stage of the iteration, due to the diversity of the population individuals, the crossover operator changes greatly, and the individuals with smaller ranking values occupy the vast majority of the next-generation individuals. As the number of iterations increases, individuals in the population tend to the same nondominated solution set, and the crossover operator will continue to approach 0.5, which will increase the searching ability of the space to a certain extent:

$$\alpha_A = \frac{\text{Rank}_A}{\text{Rank}_A + \text{Rank}_B}, \tag{16}$$

$$\alpha_B = \frac{\text{Rank}_B}{\text{Rank}_A + \text{Rank}_B}, \tag{17}$$

where Rank_X is the nondominated rank of individual X. Then, the crossover process is given in the following equations:

$$X_A^{t+1} = \alpha_A X_A^t + (1-\alpha_A) X_B^t, \tag{18}$$

$$X_B^{(t+1)} = (1-\alpha_B) X_A^t + \alpha_B X_B^t. \tag{19}$$

3.2.3. Mutation Operator. Mutation is a genetic operator used to maintain genetic diversity from one generation of a population to the next. However, the mutation probability of the traditional NSGA-II is fixed. An adaptive factor of the mutation operator equation (20) is introduced to enhance the search ability and guarantee the population density. At the early stages of the evolution, the introduced operator will promote the global optimization and will better prevent convergence to local optimum in the late evolution:

$$P_m(i) = \frac{i}{\text{gen}} * P_m. \tag{20}$$

3.3. Main Loop of the Algorithm. Considering the methods introduced above, the main loop of the proposed improved NSGA-II (Algorithm 1) is shown in Figure 7.

4. Experiments and Discussion

The datasets in this paper are from the SS-0997 train in Taiyuan North Locomotives in China. The removal of the dirty data and outliers was discussed in Section 2.1. All the experiments are implemented with MATLAB (R2014a, the MathWorks Inc., USA) in Windows 7. A nonoptimized wheel reprofiling strategy and optimization algorithm are both discussed.

4.1. Nonoptimized Wheel Reprofiling Strategy. This section will give the results of the fixed reprofiling strategy and randomly generated reprofiling strategy without the optimized wheel reprofiling strategy.

The fixed reprofiling strategy (28 and 34), which is used in current wheel reprofiling, is first simulated in this paper, and the results are shown in Figure 8. The blue solid line is the change in the flange thickness, while the red dashed line is that of the wheel diameter. The results show that the serving years of this strategy are 4.42, and the repair frequency is 3, which is close to the real operation parameters of the train.

The flange thickness is then divided into 0.5 millimeter segments to simulate different fixed strategies. Figure 9(a)

Step 1: generate a random parent population of size *nPop*.
Step 2: create a new population with the proposed selection method.
Step 3: mix the parents and children together and calculate the objective values.
Step 4: find the Pareto fronts using nondomination sorting.
Step 5: calculate the global crowding distance of the individuals.
Step 6: generate a new parent population with nondomination sorting and the global crowding distance.
Step 7: if the iteration is larger than the threshold, go to 8; otherwise, go to 2.
Step 8: find the Pareto fronts using nondomination sorting.

Algorithm 1: Improved NSGA-II.

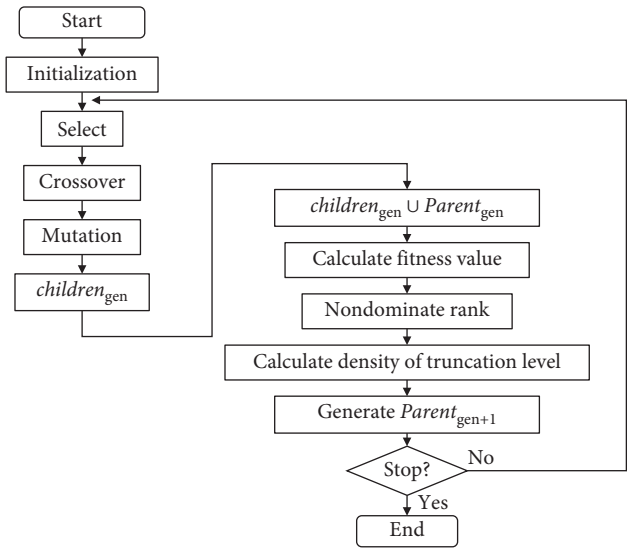

Figure 7: Flow chart of the algorithm.

Figure 8: Wear procedure of the strategy (28, 34).

shows all the strategies in this work. The points labeled o are the starting values of the reprofiling method T_i, while the points labeled * are the turning back values $T_i^{'}$. During the simulation, each time when the flange thickness is less than T_i, the wheel will be reprofiled to $T_i^{'}$. This process will be repeated until the diameter is less than 1150 millimeters.

The lifespan and the reprofiling numbers of the 78 different reprofiling strategies are shown in Figures 9(b) and 9(c), respectively. Detailed information of several preferable solutions is shown in Table 2. Column 1 in Table 2 is the reprofiling strategy, which is presented in different combinations of T_i and T_i'. Columns 2 and 3 are the serving years and reprofiling numbers, respectively. The last column is the increased proportion of the serving years compared with the current reprofiling strategy in row 1.

In Table 2, we find that, with the decrease in the recovery of flange thickness, the reprofiling times will increase. Meanwhile, with the increase in the reprofiling times, the using life years show a trend of increasing first and then decreasing. This phenomenon is most likely due to the excessive number of reprofilings, which will lead to an increase in the amount of the wheel diameter that is removed and ultimately reduce the wheel lifetime. Additionally, this rule verifies the reasonableness of the model built in Section 2.

In addition, the random generated reprofiling strategy is considered here. This strategy will generate different reprofiling strategies each time, and the detailed results are shown in Figure 10. The triangular and circular polylines represent the flange thickness before and after reprofiling, respectively, and the histogram shows the corresponding using life and repair times.

The reprofiling strategy (28.7, 33.1), (30.7, 32.1), (29.2, 29.6), (28.5, 33.1), and (28.8, 33.1) is considered the best solution among all the solutions, with the serving years being 5.8326 and the repair frequency being 5. Compared with the results of the fixed reprofiling approach, we find that the lifetime of the random strategy is an improvement. In particular, the optimal solution is 1.8% higher than that of the fixed scheme, which is approximately 36.4% higher than that of the 28 and 34 strategies. As the two experiments have not used the optimization algorithm, its accuracy and search scope are lacking, which shows the necessity of the optimization algorithm in these cases.

4.2. Optimized Wheel Reprofiling Strategy. The multiobjective optimization algorithms, the NSGA-II and improved NSGA-II, are applied to solve the reprofiling problem in this section.

Figure 11 shows the result of NSGA-II. A larger reprofiling number will decrease the availability of the wheels and increase the maintenance costs. The solutions with reprofiling numbers less than 10 in the first front are presented in Figure 11. Large reprofiling times will reduce

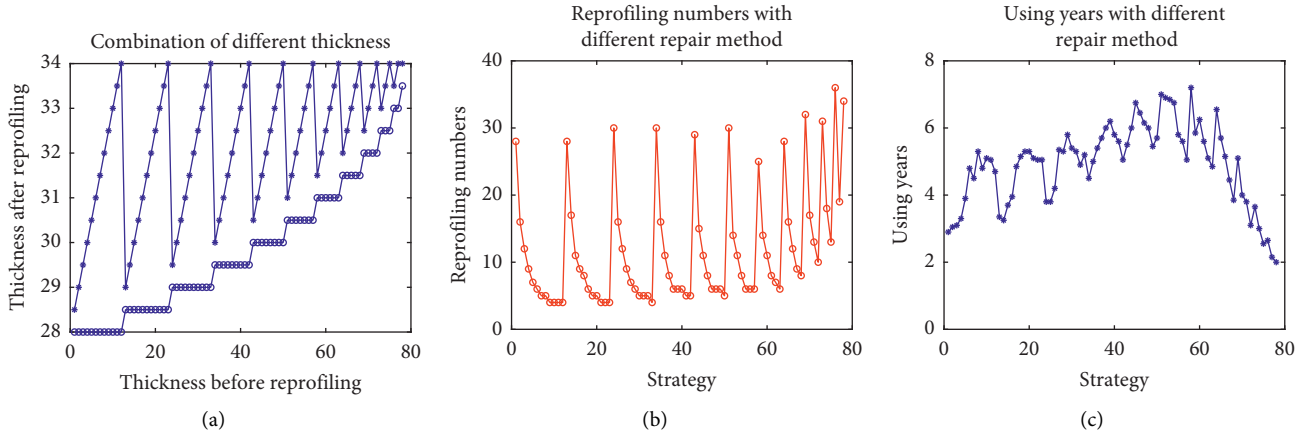

Figure 9: Results of the fixed reprofiling strategy: (a) strategy; (b) reprofiling numbers; (c) using years.

Table 2: Details of several preferable solutions.

(T_i, T_i')	Serving years	Reprofiling numbers	Increased proportion
(28.0,34.0)	4.6438	3	—
(29.0, 34.0)	5.1664	4	11.21%
(30.0, 34.0)	5.7123	5	23.0%
(29.5, 32.5)	6.2192	6	33.2%
(29.0, 31.5)	5.3151	7	14.5%
(30.5, 32.5)	6.7397	8	45.1%
(29.0, 31.0)	5.3425	9	15.4%

the wheel life and increase the maintenance costs; thus, the strategy with less than 10 reprofilings in the Pareto frontier is shown in Figure 12.

The lifecycle of the wheel will increase to 7 (50.7% increase) when the reprofiling number is 9. Compared with the currently used strategy in the first row, NSGA-II finds a better strategy that guarantees the wheel running for 5.2055 years (12.1% increase) with only one more reprofile.

The interpretation of Figure 12 is the same as Figure 10. Comparing the reprofiling times and the service life, it can be found that the average growth rate of the service life was gradually reduced from 9% to 5% with the increase in the repair times. At the same time, the NSGA-II algorithm is found to be superior to the randomly generated results, and the number of searchable solutions increases from four to five due to the use of the optimization strategy. This section considers the strategy with 7 reprofiling times and finds that 6.88 years is the best. In addition, the service life of the wheel can be increased to 7.09 years or approximately 11.80 years with 60% operation time for the entire year. The serving years using this strategy is approximately 52.51% higher than that of the current fixed strategy. Furthermore, NSGA-II found a strategy with a life of 5.47 serving years, an increase of approximately 23.59%, with only one more repair than the current Chinese repair strategy.

The improved NSGA-II proposed in Section 3 is considered here as well, and the results are shown in Figure 13. The solutions with reprofiling numbers less than 10 in the first front are presented in Figure 14. The strategy (29.9, 33.1), (30.8, 32.9), (29.3, 30.4), (29.1, 32.1), and (29.3, 32.9) with 6.73 years is considered to be a good answer.

The interpretation of Figure 14 is the same as Figure 10. The results of the improved NSGA-II have been greatly improved compared with the results of the classic NSGA-II. First, the number of solutions reprofiling times less than 10 is higher than that of the classic NSGA-II, and the proportion of available solutions increases from 27.8% to 41.2%. Second, the serving life of the improved NSGA-II is increased by an average of approximately 0.5 years (actually approximately 0.9 years) compared to the classical NSGA-II under the same number of repairs. Thus, the improved NSGA-II algorithm not only has further expanded the search range and scope but also is more targeted and effective.

4.3. Comparison and Discussion. The experimental results will be analyzed from four aspects: quality evaluation, convergence, effect, and application range.

4.3.1. Quality Evaluation. In order to compare the performance of classical NSGA-II and the improved NSGA-II algorithm, we chose the ZDT series of problems [16] (ZDT1, ZDT2, ZDT3, ZDT4, and ZDT6) as the test questions in the experiment. In the experiment, IGD (inverted generational distance) [17] is used to evaluate the quality of the algorithm. In the quality comparison of multiobjective evolutionary algorithms, IGD is one of the most commonly used performance indicators. It measures the average distance between all individuals in the true Pareto optimal set and the nearest individual in the solution set obtained by the algorithm and can provide information about the convergence of the final solution set to the true Pareto front and the diversity of the solution set. Formally, given a solution set A

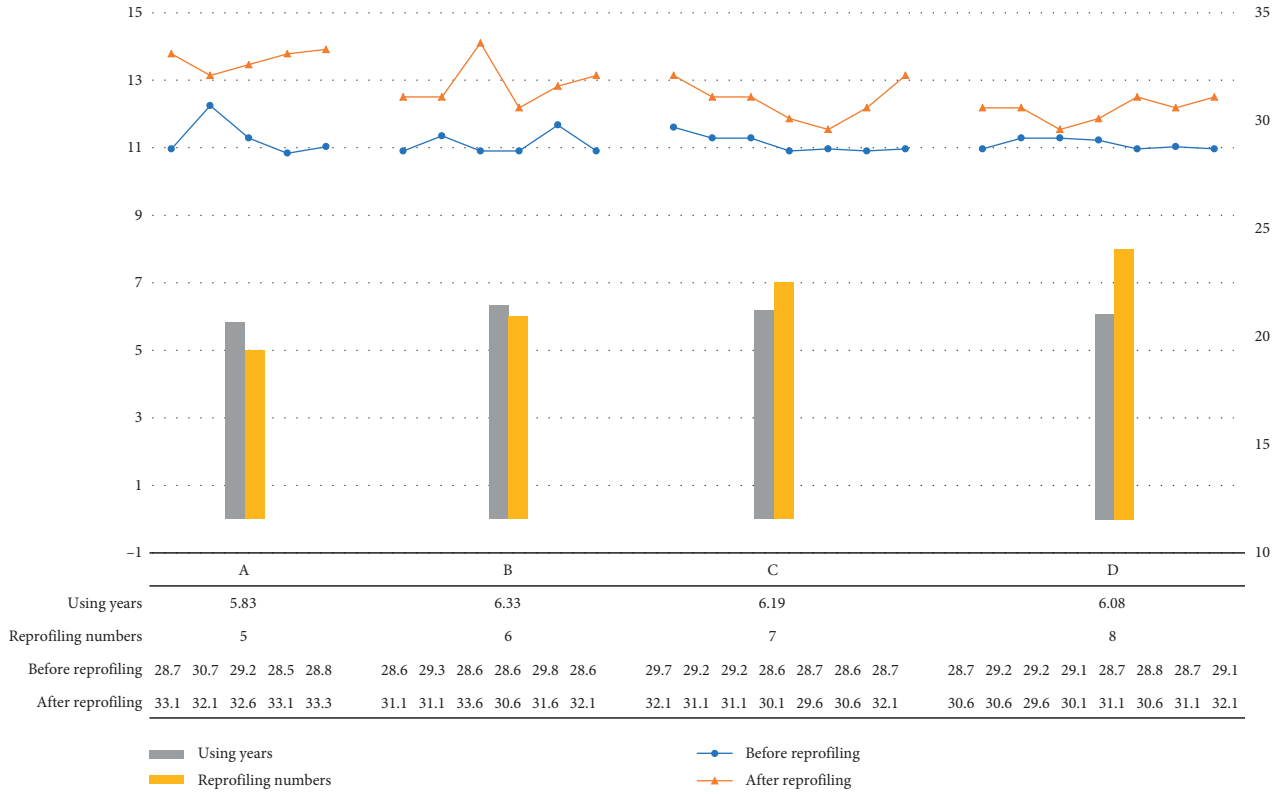

Figure 10: Random generated strategy.

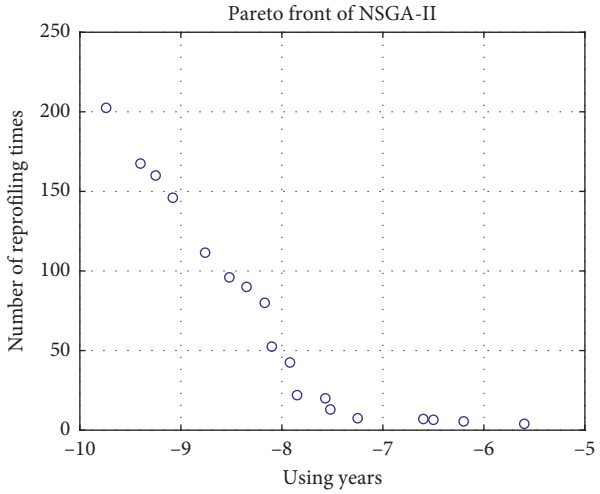

Figure 11: Results of NSGA-II.

and a reference set $R = \{r_1, r_2, \ldots, r_m\}$, IGD can be calculated by the following equation [18]:

$$\mathrm{IGD}(A, R) = \frac{1}{M} \sum_{i=1}^{M} \min_{a \in A} d_2(r_i, a), \tag{21}$$

where $d_2(r_i, a)$ denotes the Euclidean distance between r_i and a. A low IGD value indicates a better solution set. In the experiment, the population size was set as 50 and the generation as 1000, and the IGD value was calculated according to equation (21). The results are shown in Table 3.

It can be seen from the table that the IGD value of the improved NSGA-II algorithm is lower than the value of the classical NSGA-II algorithm in most ZDT problems, except for the ZDT3 problem. The overall performance of the improved NSGA-II algorithm for solving two-dimensional multiobjective problems is higher than that of the classical NSGA-II algorithm.

4.3.2. Convergence Properties. To compare the convergence properties of the classical and improved NSGA-II algorithms, the average using years of all strategies with less than 10 repair times in each iteration are plotted, as shown in Figure 15.

The abscissa in Figure 15 indicates the number of iterations, and the ordinate is the average service life. As seen from the figure, the classical NSGA-II has a fast rise at the beginning due to the randomness of the initial value and continues to oscillate approximately 5.4 years; thus, the convergence effect is not obvious. In the improved NSGA-II algorithm, because of the change in the genetic operators and global crowded density, the convergence curve increases obviously at the beginning and tends to converge at the 120th generation.

Meanwhile, the results of the improved NSGA-II are much better compared with the classical ones due to the genetic operators. First, for the convergence value, the classical NSGA-II reaches 5.4 years while the improved NSGA-II reaches 6.4 years. Second, under the same number of reprofilings, the improved NSGA-II has a longer lifespan

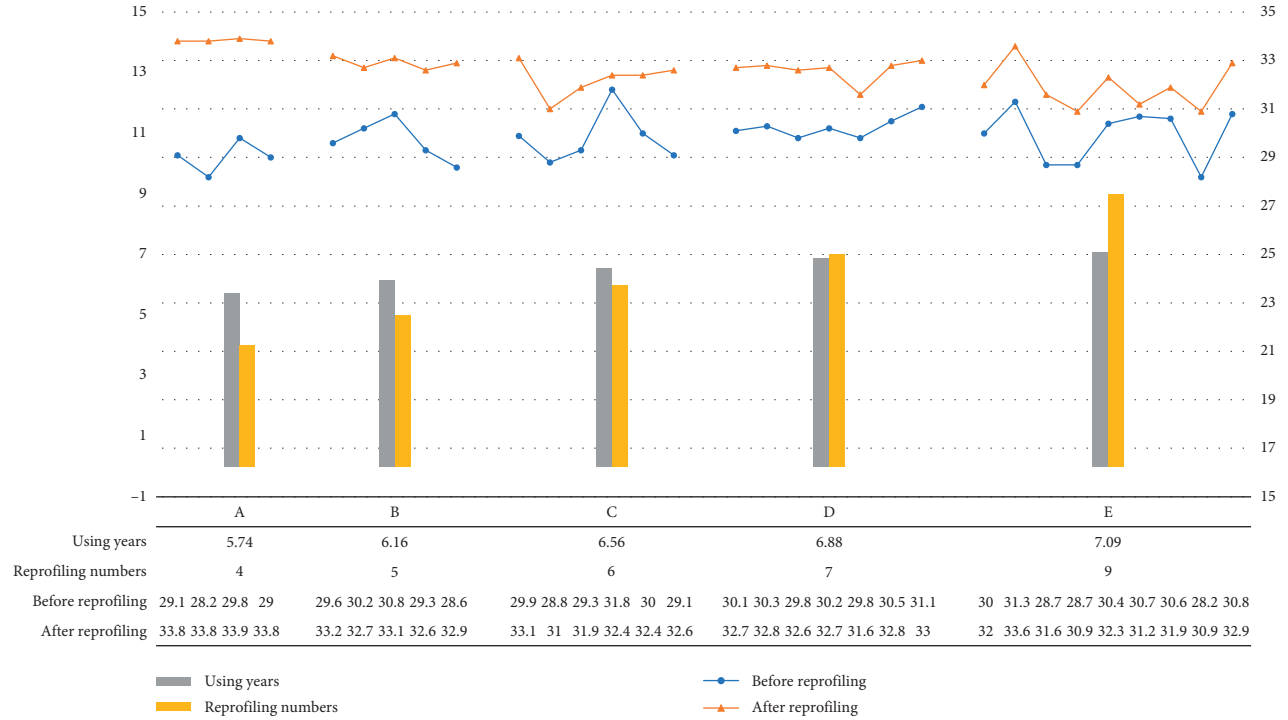

Figure 12: NSGA-II strategy.

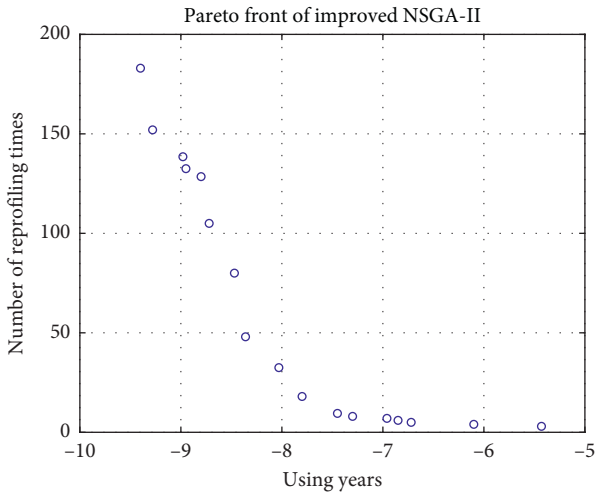

Figure 13: Results of the improved NSGA-II.

than the classical NSGA-II. Furthermore, although the Pareto frontier solution numbers of the two algorithms are both 17, the improved algorithm has searched 41.18% feasible solutions, which is higher than the classical algorithm by 13.40%.

Thus, the improved NSGA-II is not only superior to the classical NSGA-II in terms of convergence but also in search depth and breadth.

4.3.3. Algorithm Implementation Effects. Figure 16 shows the service life under the same number of reprofilings with different methods. In Figure 16, when the number of reprofilings reaches 6, the service life of the fixed repair strategy and the randomly generated strategy decrease, and the growth of service life with the optimization approaches improves slowly. The reason for this phenomenon may due to the mechanism of reprofiling. Therefore, reprofiling times should be as small as possible in real life.

After analyzing all the strategies, when the repair strategy contains 30 and 32.5, the service life will be relatively longer. This verifies the wear model obtained in Section 2.2 and helps to conclude that the SS4-0997 locomotive wheel reprofiling strategy should include 30 and 32.5. When considering the performances of the four approaches, the proposed algorithm outperforms NSGA-II, while NSGA-II is better than other simulation approaches. This is important when applying the reprofiling strategies listed in this paper by maintenance engineers.

With all the strategies, the improved algorithm has a service life increase from 4.64 years to 5.232 years (14.66%) under 3 reprofilings (the same as the current one). Comprehensive consideration of repair and wheel replacement costs, (29.9, 33.1), (20.8, 32.9), (29.3, 30.4), (29.1, 32.1), and (29.3, 32.9), found by the proposed algorithm is considered to be the best strategy in this paper with 5 reprofiling times and 6.73 serving life years, which is approximately 45.04% higher than the current strategy.

5. Application Range of the Algorithm

From the practical application of the algorithm, on the one hand, the proposed algorithm is suitable for producing the reprofiling schedule for any wheel in SS4-0997 locomotives. On the other hand, in the ideal locomotive operating environment, which does not need to consider the wheel

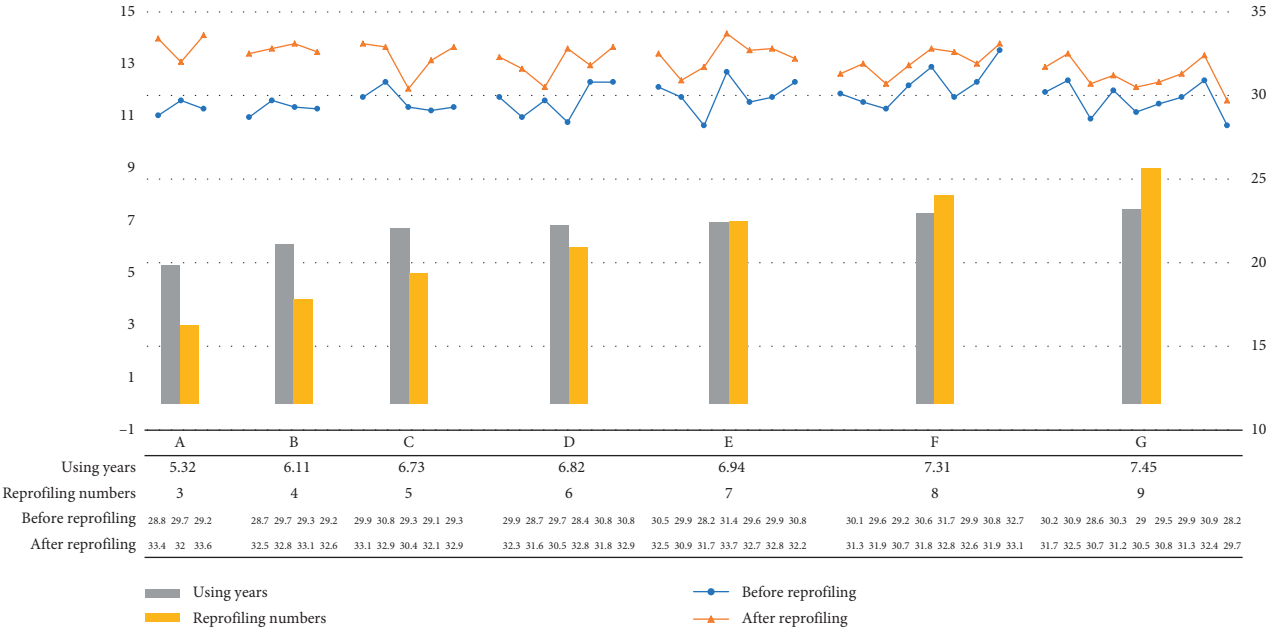

Figure 14: Random generated strategy.

Table 3: IGD value of ZDT series of problems.

Test problem	Classical NSGA-II	Improved NSGA-II
ZDT1	$2.391929e-03$	**$2.082921\ e-03$**
ZDT2	$2.710113e-03$	**$2.492973\ e-03$**
ZDT3	**$1.486839\ e-02$**	$1.506779e-02$
ZDT4	$5.646924e-02$	**$3.156867\ e-02$**
ZDT6	$4.589117e-02$	**$3.598761\ e-02$**

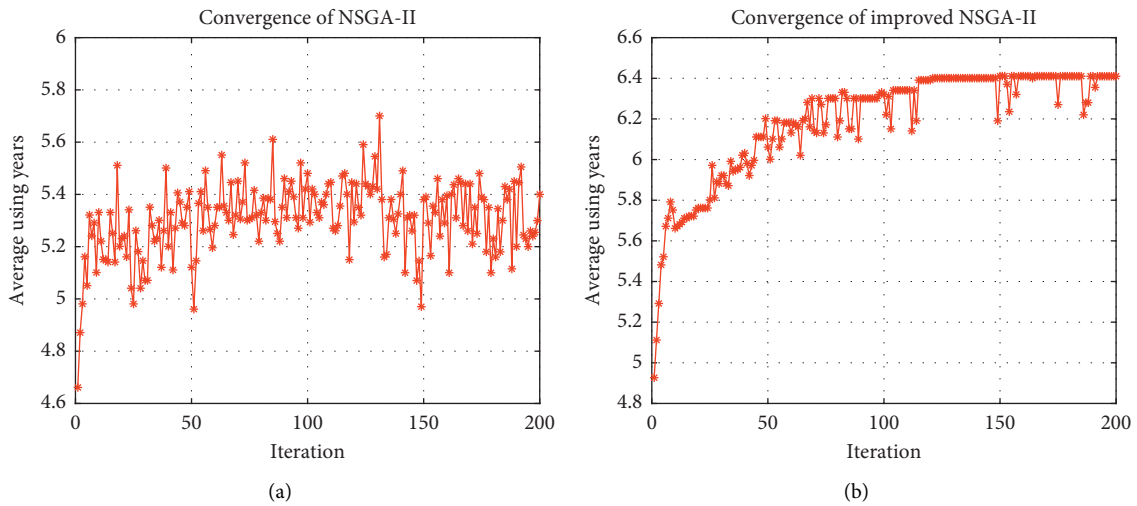

Figure 15: Convergence of the algorithms. (a) Classical NSGA-II. (b) Improved NSGA-II.

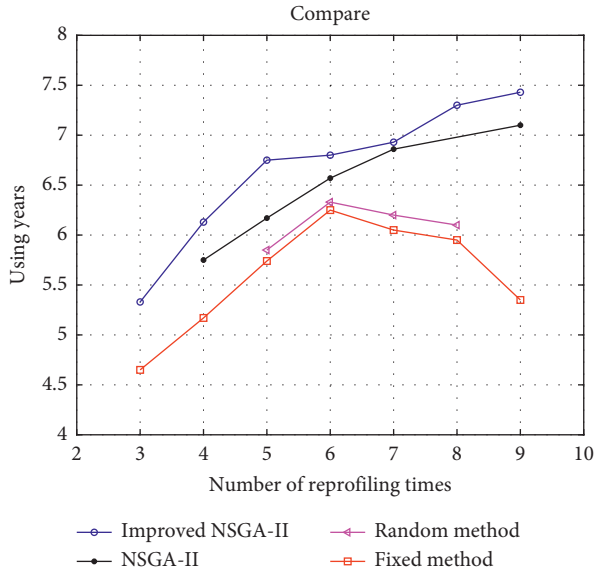

Figure 16: Service life.

diameter difference, the proposed algorithm can be used to make the vehicle repair plan.

6. Conclusions

In this work, the wear model and multiobjective model of the reprofiling are introduced. An improved NSGA-II with the change in the crowding distance calculation and genetic operators is proposed to better fit the proposed multiobjective model. Datasets from the SS-097 trains in the Taiyuan North Locomotive are used to illustrate the effectiveness of the proposed approach. The results show that improved NSGA-II performs better than NSGA-II, and NSGA-II performs better than the simulation approaches. The best reprofiling strategy (29.9, 33.1), (31.8, 31.9), (29.3, 29.4), (29.1, 30.1), and (29.3, 29.9) with 6.5342 serving years and a repair frequency of 5 is better than the strategy (28.0, 34.0) currently used (4.6438 serving years and repair frequency of 3). Therefore, the strategy can significantly increase the existing reprofiling strategy of the Taiyuan locomotive depot in China. It is possible that the models and approaches presented here are not suitable for other wheels. However, the study in this paper provides new insights into solving the reprofiling problem.

There are several recommendations for further studies: focusing on reprofiling strategies of wheels for a carriage with 16 wheels, taking the reprofiling gain into account, and developing a system to analyze each wheel based on the proposed model.

Data Availability

The data used to support the findings of this study are available from the corresponding author upon request.

Conflicts of Interest

The authors declare that they have no conflicts of interest.

Acknowledgments

This work was supported by funding from the National Natural Science Foundation of China (Grant no. 61571226).

References

[1] R. H. Fries and C. G. Dávila, "Analytical methods for wheel and rail wear prediction," *Vehicle System Dynamics*, vol. 15, no. 15, pp. 112–125, 1986.

[2] R. Enblom and M. Berg, "Impact of non-elliptic contact modelling in wheel wear simulation," *Wear*, vol. 265, no. 9-10, pp. 1532–1541, 2008.

[3] X. U. Hong, "Modeling of metro wheel wear and optimization of the wheel re-profiling strategy based on Gaussian processes," *Journal of Mechanical Engineering*, vol. 46, no. 24, pp. 88–95, 2010.

[4] R. Enblom and B. Dirks, "Prediction model for wheel profile wear and rolling contact fatigue," *Wear*, vol. 271, no. 1, pp. 210–217, 2011.

[5] J. J. Ding, S. L. Sun, L. I. Fu, and Y. H. Huang, "Simulation of wheel wear for heavy haul freight car," *Journal of Traffic & Transportation Engineering*, vol. 11, no. 4, pp. 56–60, 2011.

[6] B. Zhang, L. U. Zhenggang, and T. Chen, "Wheel reprofiling of high-speed emu based on multi-objective optimization strategy," *Journal of Tongji University*, vol. 41, no. 3, pp. 437–442, 2013.

[7] G.L. Liao, *Research on the Security State Prediction and Lathing Strategy Optimization for the Wheelset of Urban Rail Train*, Beijing Jiaotong University, Beijing, China, 2014.

[8] L. Wang, H. Xu, H. Yuan, W. Zhao, and X. Chen, "Optimizing the re-profiling strategy of metro wheels based on a data-driven wear model," *European Journal of Operational Research*, vol. 242, no. 3, pp. 975–986, 2015.

[9] K. Deb, A. Pratap, S. Agarwal, and T. Meyarivan, "A fast and elitist multiobjective genetic algorithm: NSGA-II," *IEEE Transactions on Evolutionary Computation*, vol. 6, no. 2, pp. 182–197, 2002.

[10] D. W. Corne, J. D. Knowles, and M. J. Oates, "The pareto envelope-based selection algorithm for multiobjective optimization," in *Proceedings of the International Conference on Parallel Problem Solving from Nature*, September 2000.

[11] E. Zitzler, M. Laumanns, and L. Thiele, "SPEA2: improving the strength Pareto evolutionary algorithm for multiobjective optimization," in *Proceedings of the Evolutionary Methods For Design, Optimization and Control with Applications to Industrial Problems*, Athens, Greece, September 2001.

[12] D. Martĺłn, A. Rosete, J. Alcalĺć -Fdez, and F. Herrera, "QAR-CIP-NSGA-II: a new multi-objective evolutionary algorithm to mine quantitative association rules," *Information Sciences*, vol. 258, no. 3, pp. 1–28, 2014.

[13] F. Pascual and J. A. Marcos, "Wheel wear management on high-speed passenger rail: a common playground for design and maintenance engineering in the talgo engineering cycle," in *Proceedings of the 2004 ASME/IEEE Joint Rail Conference*, pp. 193–199, Baltimore, MD, USA, April 2004.

[14] H. Yuan and S. Xiao, *Feasible Analysis of Wheelset Class-Lathing on the Statistics of Wheelset Wearing*, Urban Mass Transit, Mayur Vihar, India, 2006.

[15] A. Rodriguez and A. Laio, "Machine learning. clustering by fast search and find of density peaks," *Science*, vol. 344, no. 6191, pp. 1492–1496, 2014.

[16] E. Zitzler, L. K. Deb, and L. Thiele, "Comparison of multiobjective evolutionary algorithms: empirical results," *Evolutionary Computation*, vol. 8, no. 2, pp. 173–195, 2000.

[17] E. Zitzler and Thiele, "Performance assessment of multiobjective optimizers: an analysis and review," *IEEE Transactions on Evolutionary Computation*, vol. 7, no. 2, pp. 117–132, 2003.

[18] M. Li and X. Yao, "Quality evaluation of solution sets in multiobjective optimisation," *ACM Computing Surveys*, vol. 52, no. 2, pp. 1–38, 2019.